Petroleum Science (2019) 16:578–590
https://doi.org/10.1007/s12182-019-0314-x

ORIGINAL PAPER

Experimental investigation into Fe_3O_4/SiO_2 nanoparticle performance and comparison with other nanofluids in enhanced oil recovery

Yousef Kazemzadeh[1] · Behnam Dehdari[2] · Zahra Etemadan[2] · Masoud Riazi[2] · Mohammad Sharifi[1]

Received: 7 April 2018 / Published online: 15 April 2019

Abstract

Nanofluids because of their surface characteristics improve the oil production from reservoirs by enabling different enhanced recovery mechanisms such as wettability alteration, interfacial tension (IFT) reduction, oil viscosity reduction, formation and stabilization of colloidal systems and the decrease in the asphaltene precipitation. To the best of the authors' knowledge, the synthesis of a new nanocomposite has been studied in this paper for the first time. It consists of nanoparticles of both SiO_2 and Fe_3O_4. Each nanoparticle has its individual surface property and has its distinct effect on the oil production of reservoirs. According to the previous studies, Fe_3O_4 has been used in the prevention or reduction of asphaltene precipitation and SiO_2 has been considered for wettability alteration and/or reducing IFTs in enhanced oil recovery. According to the experimental results, the novel synthesized nanoparticles have increased the oil recovery by the synergistic effects of the formed particles markedly by activating the various mechanisms relative to the use of each of the nanoparticles in the micromodel individually. According to the results obtained for the use of this nanocomposite, understanding reservoir conditions plays an important role in the ultimate goal of enhancing oil recovery and the formation of stable emulsions plays an important role in oil recovery using this method.

Keywords Enhanced oil recovery · Asphaltene precipitation · Wettability alteration · Interfacial tension reduction · Fe_3O_4/SiO_2 nanofluid

1 Introduction

Primary and secondary techniques for in situ oil production and recovery are weak and fragile methods; hence, special attention has been paid toward more efficient modern technologies such as nanotechnology for enhancing oil recovery of reservoirs (Aminzadeh et al. 2013; Moghadam and Azizian 2014; Zhang et al. 2010). On average, about one-third of initial in situ oil can be produced via primary and secondary methods. The remaining oil has been trapped in pores in the reservoir rock due to the surface and interfacial forces (Kumar and Mandal 2018). This oil may be pulled out by reducing the capillary forces which prevent the movement of oil in reservoir pores (Kazemzadeh et al. 2015; Krevor et al. 2015; Liu et al. 2012). The overall efficiency of each enhanced oil recovery method includes microscopic and macroscopic efficiencies (Al Adasani and Bai 2011; Cheraghian and Hendraningrat 2016b). The former is attributed to the movement of oil on the pore scale, and the latter is related to the volume of the displacing fluid in the reservoir (Steeb et al. 2012). A micromodel is an artificial two-dimensional porous medium used to simulate the porous medium on the pore scale (Zhang et al. 2011). The force required to compress small hydrocarbon droplets trapped in pore throats can be provided by the capillary force which can be diminished by a decrease in interfacial tension or wettability alterations (Al-Anssari et al. 2016; Kazemzadeh et al. 2015; Krevor et al. 2015). Nanoparticles, on the other hand, provide a unique approach to control oil recovery (Bera and Belhaj 2016; Kazemzadeh et al. 2018b). They possess individual properties which can provide desired features such as high specific area, chemical reactivity and active surface properties (Ahmadi et al. 2016; Kazemzadeh et al.

Edited by Yan-Hua Sun

✉ Yousef Kazemzadeh
yusefkazemzade@yahoo.com; yusefkazemzade@aut.ac.ir

[1] Department of Petroleum Engineering, Amirkabir University of Technology, Tehran Polytechnic, Tehran, Iran

[2] School of Chemical and Petroleum Engineering, Shiraz University, Shiraz 7194684471, Iran

2018a; Li et al. 2017). The relevant formation sizes are from nanometer to micrometer scales. Because the nanoparticles have a diameter of 1–100 nm, they can move easily in pores in the reservoir rock due to their smaller size compared to the pore throats (Kazemzadeh et al. 2018c; Rezvani et al. 2018). Accordingly, these nanoparticles are a potential candidate for rock wettability alteration. It has been proved that nanoparticles can significantly enhance the oil production through the following mechanisms:

- Altering the viscosity of the injecting fluid (Sharma et al. 2015)
- Altering the density of the injecting fluid (Rezvani et al. 2018)
- Reducing the interfacial tension (Cheraghian and Hendraningrat 2016a; Skauge et al. 2010)
- Improving the emulsification process (Kumar et al. 2017; Patel et al. 2017)
- Improving the conductivity and specific heat (El-Diasty and Aly 2015)
- Improving the reactions between fluids and rocks (Rezvani et al. 2018)
- Altering the wettability (Rezvani et al. 2018)
- Altering the heat transfer coefficient (Nassar et al. 2011a)
- Reducing the formation damage via reducing the force on the pore surfaces (Cheraghian and Hendraningrat 2016b; El-Diasty and Aly 2015; Patel et al. 2017; Skauge et al. 2010; Wang et al. 2010).

The utilization of nanoparticles for enhanced oil recovery has achieved increasing attention although it is still at the initial stages of development. This is due to their diverse features and advantages such as:

- Small size which allows them to enter the pores and extract oil without trapping (Maurya and Mandal 2018)
- Capability to change the properties of fluids resulting in proper mobility ratios (Pourabdollah et al. 2013)
- The ability to stabilize emulsions (Maurya and Mandal 2018)
- Faster and better heat transfer in thermal enhanced oil recovery (EOR) methods (Nassar et al. 2011b)
- More compatibility with the environment than other chemical materials (Maurya et al. 2017)
- High temperature and pressure tolerance due to their higher decomposition resistance than other materials (Nassar et al. 2011a).

Moreover, nanoparticles can inhibit asphaltene precipitation (Kazemzadeh et al. 2015). They are also able to remove asphaltene precipitations from the surface due to their thermal catalytic role. Hence, the role of nanoparticles can be divided into two parts (Doryani et al. 2016). Firstly, they can quickly attract asphaltene particles due to their high capacity of adsorption which, in turn, results in a greater mobility of oil and prevents asphaltene accumulation (Parsaei et al. 2017). Secondly, wettability alteration of oil-wet reservoir rocks is of practical importance since the rock wettability alteration to water wet allows injection water to efficiently penetrate into pores, before reducing water relative permeability. Thus, a more favorable mobility ratio and a higher recovery factor are anticipated. Driving oil from smaller pores to larger ones and increasing oil production are the results of higher water tendency to adhere to formation surfaces than oil.

Several studies have been conducted in the field using nanoparticles for improving conditions for oil production from reservoirs. Ogolo et al. (2012) have claimed some nanoparticles can improve productivity, and this effect is improved in the presence of ethanol. They have also expressed the mechanisms by which nanoparticles can improve the productivity due to wettability alteration, interfacial tension (IFT) reduction, oil viscosity reduction, decline in mobility ratio and permeability alteration (Ogolo et al. 2012). Application of nanofluids in enhanced oil recovery was investigated by Suleimanov et al. (2011) using metal nanoparticles. They have revealed that a nanoparticle–surfactant system can enhance oil recovery up to 35% while the enhanced recovery was measured to be 17% in a system that only contained surfactants. This was attributed to the decline in the interfacial tension in the presence of nanoparticles (Suleimanov et al. 2011). Roustaei et al. (2012) have also studied the efficiency of poly-silicon nanoparticles by measuring the interfacial tension and contact angle. They have discovered that the surface tension is considerably diminished, and oil production is significantly enhanced using nanoparticles (Roustaei et al. 2012). Wei et al. used a modified nanofluid to improve oil production from oil reservoirs. This was carried out in two ways: (1) improvement in volume sweep efficiency and (2) emulsification and entrainment. They also suggested this fluid can be utilized as an ameliorative fluid in flooding in the near future (Wei et al. 2016). In another effort, Hendraningrat et al. (2013) have studied the efficiency of suspended solutions containing hydrophilic poly-silicon nanoparticles. They have reported a decline in the interfacial tension between water and oil in the presence of nanofluids and the fact that the solid surface became more water wet. They eventually measured about 5% additional oil recovery in the presence of nanoparticles (Hendraningrat et al. 2013). Pei et al. (2015) have investigated the increase in stability of emulsions under the effect of nanoparticles in micromodel experiments. Their findings have proved the capability of nanoparticles to increase the thickness of the emulsion layer and improve the mobility ratio. The existing heavy oil also becomes emulsified during the injection of surfactant–nanoparticle-stabilized

Table 1 Properties of the crude oil used

Oil gravity, °API	Density at 25 °C, g/mL	Viscosity at 25 °C, cP	SARA composition, wt%			
			Saturates	Aromatics	Resins	Asphaltenes
21.49	0.9249	145.1	40.85	48.79	7.71	2.61

Table 2 Composition of the crude oil

Component	C_2	C_3	i-C_4	n-C_4	i-C_5	n-C_5	C_6	C_7	C_8	C_9	C_{10}	C_{11}	C_{12+}
Content, mol%	0.49	0.73	0.47	0.94	0.55	0.55	7.64	6.18	5.44	4.90	4.71	4.14	63.26

Table 3 Properties and compositions of reservoir brine and seawater used

Water	Ion composition, ppm							Total dissolved solids, ppm	pH
	Na^+	K^+	HCO_3^-	Ca^{2+}	Mg^{2+}	Cl^-	SO_4^{2-}		
Formation water	67,550	1187	989	7400	1575	122,945	424	202,070	6.24
Seawater	18,780	727	229	1250	1500	302	3360	26,148	7.39

emulsions. They have claimed that such emulsions which were stabilized by nanoparticles and surfactants can produce 40% of the in situ oil in the enhanced oil recovery process (Pei et al. 2015).

In this study, the influence of a novel nanocomposite on enhanced oil recovery from reservoirs is investigated using a two-dimensional micromodel taken from the actual structure of the reservoir rock. Nanoparticles contribute to activating different EOR mechanisms based on their individual physical and chemical structures. Nanocomposites contain various nanoparticles. The synergistic effect of nanoparticles in increasing active mechanisms of oil production can be observed in nanocomposites in the case of correct synthesis. The performance of the nanoparticles and the nanocomposite of Fe_3O_4/SiO_2 in enhanced oil recovery is evaluated and compared with other flooding scenarios.

2 Experimental

2.1 Materials

The crude oil used was from one of the southern reservoirs in Iran, and its fluid properties, SARA analysis results and composition are listed in Tables 1 and 2. Its API gravity was 21°. The asphaltene and resin contents of the crude oil were measured to be 7.71% and 2.61% by weight, respectively, which shows that its colloidal instability index (CII) value was about 0.90 and the oil was unstable in terms of asphaltene thermodynamic compounds and susceptible to precipitation. Hence, this crude oil used was heavy. The colloidal instability index (CII) defined, as below, is a benchmark for determining the instability of colloidal systems, where $w_{\text{saturated}}$, $w_{\text{asphaltene}}$, w_{aromatic} and w_{resin} are the weight percentages of the saturate, asphaltene, aromatic and resin fractions, respectively.

$$\text{CII} = \frac{w_{\text{saturates}} + w_{\text{asphaltenes}}}{w_{\text{aromatics}} + w_{\text{resins}}} \quad (1)$$

2.2 Properties of formation water and injection water

Compositions and properties of the formation water from a reservoir in the Mansoori oil field and Persian Gulf Water (used as injection water) are listed in Table 3. Moreover, the Persian Gulf Water was used to prepare all nanofluids.

2.3 Nanoparticles

Two different nanoparticles were provided by the US Research Nanomaterials (US-Nano) Co., and their general characteristics are listed in Table 4. Scanning electron microscopic (SEM) images of these nanoparticles are shown in Fig. 1.

2.4 Synthesis of Fe_3O_4/SiO_2 nanostructures

These nanostructures were synthesized by a sol–gel technique and method of Stover (Rezvani et al. 2018). Fe_3O_4 nanoparticles (1.0 g) were dispersed in a mixture of distilled water (100 mL) and ethanol (500 mL) in an ultrasonic bath for about 15 min. Ammonia solution (12 mL) and tetraethyl ortho-silicate (54.1 g) were subsequently added and stirred for about 5 h with a mechanical stirrer. The sol–gel-synthesized nanoparticles were then separated from the solution by centrifuging at 4000 rpm and were rinsed with distilled water twice (100 mL each time) and dried at 40 °C for 24 h.

Table 4 Properties of nanoparticles

Nanoparticle	Purity, %	Average diameter of solid particles, nm	Specific surface area, m^2/g	True density, g/cm^3	Color	Morphology	Chemical properties
SiO_2	99.50	15–20	640	2.40	White	Porous	Acidic
Fe_3O_4	98.00	20–30	40–60	5.00	Dark brown	Spherical	Amphoteric

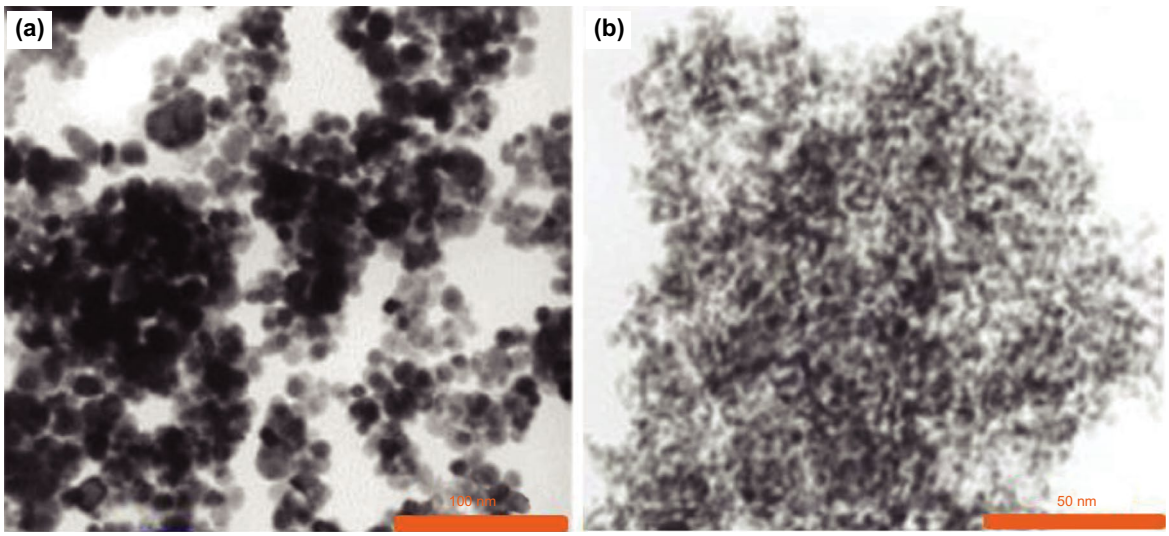

Fig. 1 SEM images of nanoparticles. **a** Fe_3O_4 and **b** SiO_2

The diffraction pattern of samples was obtained with an X-ray diffractometer (PW1840, Philips Co.) at ambient temperature. Phase detection of samples was conducted by comparing X-ray diffraction patterns and JCPDS standard data while the diffraction angle was set between 10° and 80° in the experiment. A soft and uniform layer of the sample was separated and put in the X-ray device. According to Fig. 2, the synthesized nanocomposite was characterized by peaks at 2θ values of 18°, 30°, 35°, 37°, 43°, 53°, 57° and 62°. Diffraction pattern indicates that Fe_3O_4 in the composite has a spinel crystalline structure. Based on the present pattern, no other metal oxide phases were detected in the synthesized nanoparticles.

A FE-SEM image of Fe_3O_4/SiO_2 nanostructures is shown in Fig. 3. As it can be seen from the figure, the SiO_2 coverage around the nanoparticles was about 25 nm in diameter and nanostructures were about 30 nm in size.

Magnetic nanoparticles of iron oxide are directly linked with silica, and a silicon dioxide shell is formed around the iron oxide particles. The process which forms a shell/core structure is completed through hydrolysis of a sol–gel precursor. No connector is required for the adhesion of silica to metal oxide nanoparticles due to the strong attraction of the iron oxide surface toward silica.

Fourier-transform infrared spectroscopy (FT-IR) was used for further investigation of magnetic nanostructures. An FT-IR spectrum of the Fe_3O_4/SiO_2 nanostructures is illustrated in Fig. 4.

In the FT-IR spectrum of magnetic nanoparticles (i.e., Fe_3O_4/SiO_2 nanocomposite), an absorption peak at 577.2 cm^{-1} is attributed to stretching vibration of the Fe–O bond and peaks at 3424 and 1636 cm^{-1} indicate the existence of O–H groups on the surface of nanoparticles which confirms the formation of Fe_3O_4. The stretching vibration of Si–O and Si–OH bonds is observed at 1111 and 805 cm^{-1}, respectively, which indicates the silica coverage of nanoparticles.

2.5 Micromodel

Preparing the initial pattern designs is the first and most important stage in building a glass micromodel. Designs used in this stage can be taken from the scanned structures of the rock surfaces or artificial designs similar to pores and throats of the reservoir rock. The present plan was designed with CorelDraw software. The ratio of pore sizes to throat sizes is essential due to reaching the desired capillary forces

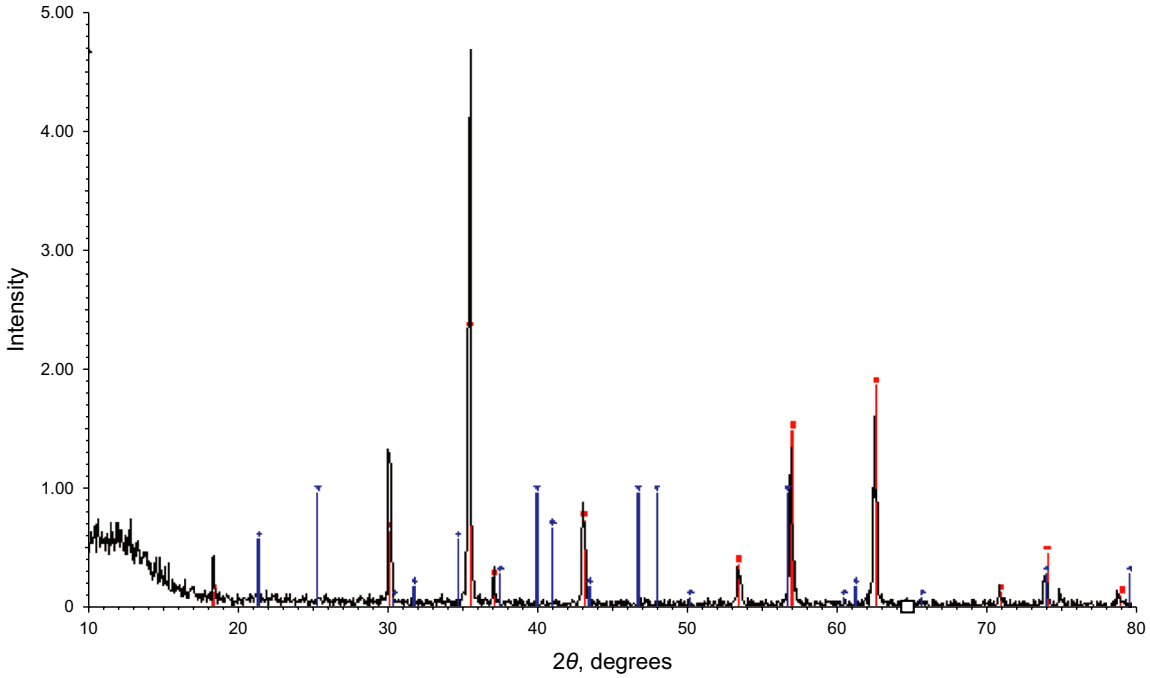

Fig. 2 X-ray diffraction (XRD) analysis of the synthesized nanocomposite

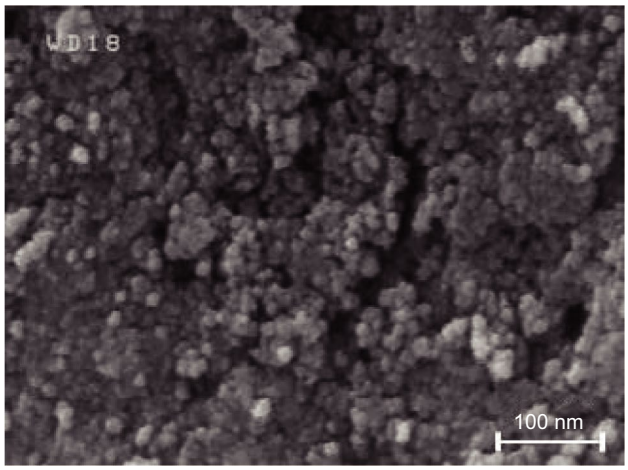

Fig. 3 FE-SEM image of the Fe_3O_4/SiO_2 nanostructures (Kazemzadeh et al. 2018b)

of the porous medium and matching with real conditions. The present plan is taken from a real reservoir rock (Fig. 5).

The plan requires it to be engraved on a glass after designing. A corrosion-resistant glue was used to engrave the design on the glass. When the glue adhered to the glass, the design was engraved on it using a laser. The glue-covered glass was subsequently put into hydrofluoric acid. A proper timing was required to form the design on the glass effectively. For this purpose, hydrofluoric acid was used in different time intervals to provide the proper corrosion. The glass was first put into the acid for 3 min and was rinsed with water for 10 min to remove the remaining acid from the glass. In the next step, the glass was again put into the acid for 3 min and thoroughly rinsed with water for another 10 min. In the third step of the etching process, the glass was kept in the acid for 4 min and rinsed with high-pressure water for 15 min. In the final step, the micromodel was kept for about 4 min in the acid and rinsed for another 4 min with water to remove the remaining acid. Now it is required to position the needle of the micromodel on it. The place of the needle was curved on the glass by high-accuracy drilling, and the needle was then adhered to the micromodel using glue. The micromodel needed to be placed in a high-temperature furnace so that two pieces of glass were properly adhered together. Overall properties of the micromodel are presented in Table 5.

2.6 Experimental setup

A system for analyzing nanoparticle performance is illustrated in Fig. 6, and a Quizix pump was used to inject fluids at very low rates. The operating rate was set to 0.5 mL/h in this study to properly simulate the laminar flow of fluids in a porous medium. A camera was set at the top of the micromodel to take pictures of the micromodel and variations in saturations and phase displacement at specific time intervals (every 1 min). Oil recovery rate and production mechanisms were inferred from the image analysis. The amount of available oil (residual oil) in the micromodel was calculated using

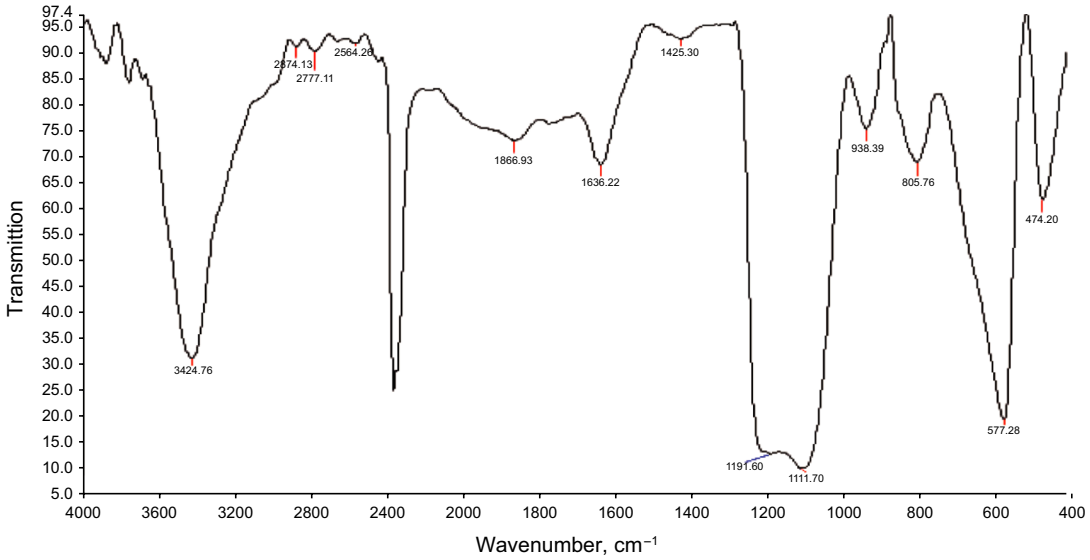

Fig. 4 FT-IR spectrum of the Fe_3O_4/SiO_2 nanocomposite

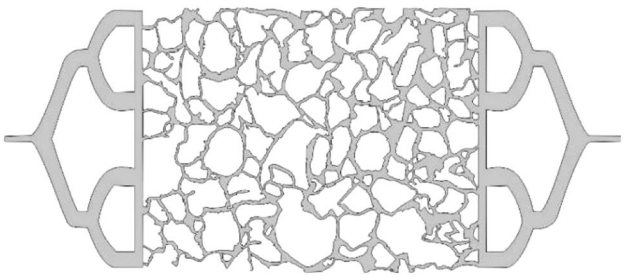

Fig. 5 Micromodel specifications

Table 5 Physical properties of the glass micromodel

Wide, cm	Length, cm	Average pore diameter, μm	Average throat diameter, μm	Porosity, %	Permeability, D
5	10	650	200	32	4

ImageJ software. As the volume of empty areas (V_p) was easily obtained, the oil recovery factor was calculated from the following equation:

$$f = \frac{V_{\text{extracted}}}{V_T} = \frac{V_T - V_{\text{residual oil}}}{V_T}$$

where f is the oil recovery factor; $V_{\text{extracted}}$ is the volume of oil extracted from the micromodel after flooding; $V_{\text{residual oil}}$ is the volume of oil trapped in the micromodel after flooding; and V_T is the total volume of oil contained in pores and throats in the event that the micromodel is saturated with oil.

The pendant drop method was adopted to measure the contact angle between glass and oil and hence wettability alterations (Fig. 7).

2.7 Method

All the methods for analyzing the processes of fluid injection into reservoirs are similar as follows:

(1) The micromodel was first rinsed with acetone and distilled water, and its surface was then altered to oil wet with 0.018 M stearic acid and normal heptane.
(2) Formation water was injected into the micromodel at a rate of 0.5 mL/h. A total of 2 PV formation water was injected into the micromodel.
(3) Oil was injected at a rate of 0.5 mL/h to saturate the micromodel.
(4) The displacing fluids (Table 6) were injected at a rate of 0.5 mL/h, and the displacing and displaced phases were imaged in this stage. The recovery coefficient and EOR mechanisms were analyzed afterward. It is worth noting that these nanofluids were prepared with seawater.

3 Results and discussion

As explained earlier in Sect. 2.7, the micromodel was first saturated with formation water, and then, crude oil was subsequently injected at a flow rate of 0.5 mL/h. The image of the oil-saturated micromodel is presented in

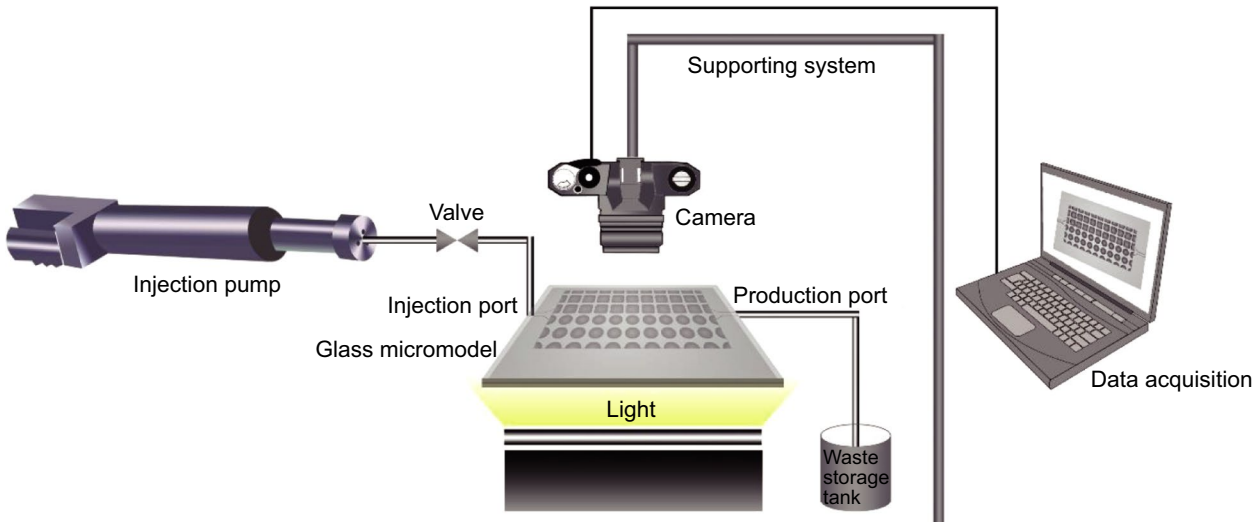

Fig. 6 Schematic view of the glass micromodel setup (Kazemzadeh et al. 2015)

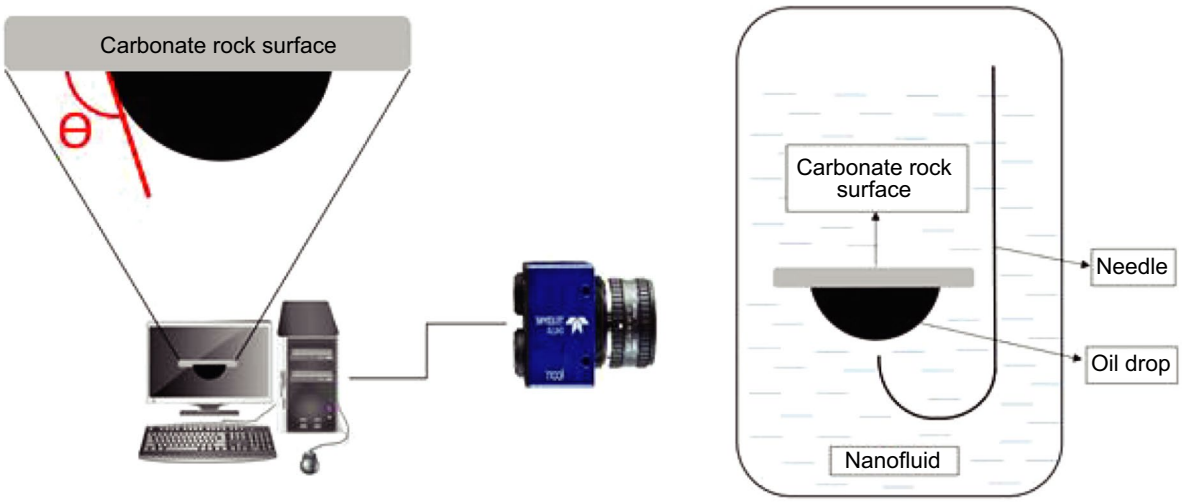

Fig. 7 Pendant drop method used for wettability assessment

Table 6 Displacing fluids used in displacement experiments

Displacing fluid	Nanoparticle concentration, wt%	Viscosity, cP
Seawater	–	1.09
SiO_2 nanofluids	0.1	1.17
Fe_3O_4 nanofluids	0.1	1.15
Fe_3O_4/SiO_2 nanofluids	0.1	1.19

Fig. 8 Oil-saturated micromodel showing the remaining water (white color) after oil injection

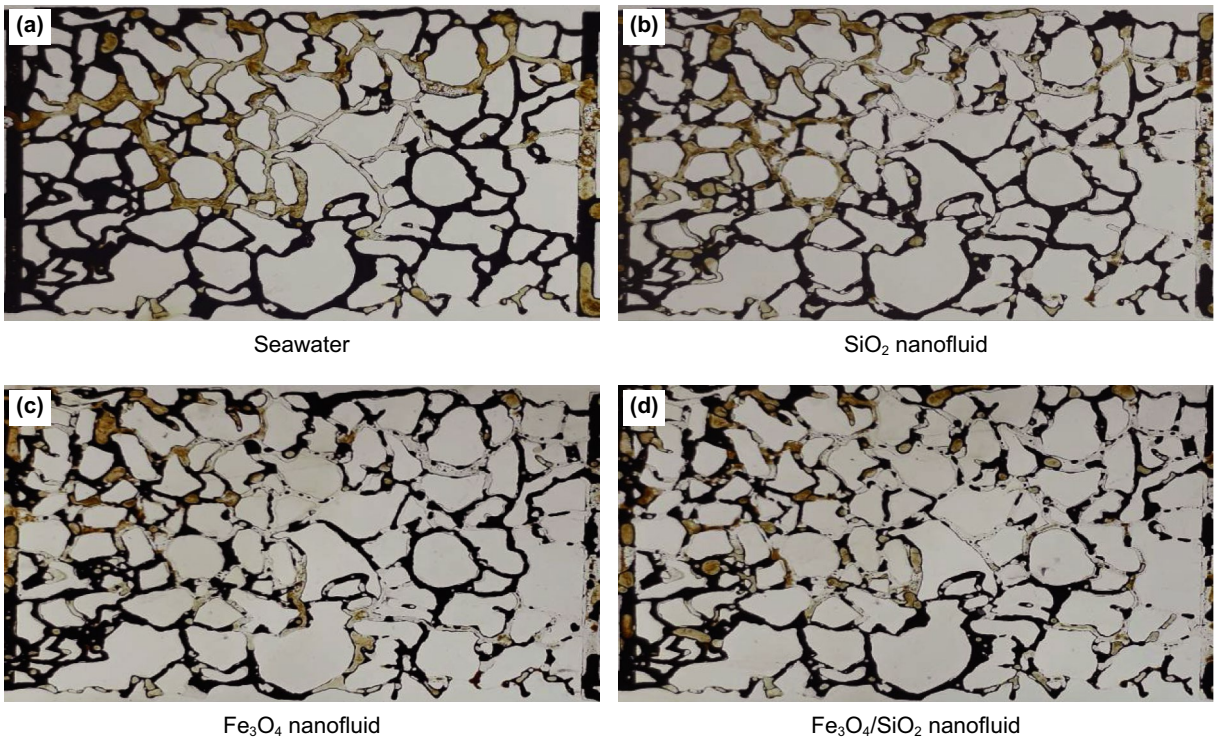

Fig. 9 Micromodel images after 240 min of different displacing fluid injections

Fig. 8. The black, white and brown colors represent oil, water and emulsion, respectively.

As it can be seen in Fig. 8, the micromodel was saturated with oil and a little formation water, i.e., connate water, was trapped and remained in pores and throats.

After oil injection, each of the four mentioned fluids in Table 6 is injected separately into the micromodel at a flow rate of 0.5 mL/h. The micromodel saturation profiles were recorded after 240 min of fluid injection, as shown in Fig. 9. The brown color liquid is emulsions formed between formation water and oil.

The final oil recovery depends on various parameters. Besides the governing mechanisms in the injection process, asphaltene precipitation and formation of oil-in-water and water-in-oil emulsions affect the final oil recovery. The oil used was susceptible to precipitation; therefore, asphaltene precipitation could be observed at throat mouths in the porous medium in the injection process. Asphaltene precipitation could alter the wettability of the glass and change the moving direction of the displacing fluid by clogging the pores (Doryani et al. 2016, 2018; Kazemzadeh et al. 2015). The formation of oil-in-water emulsions was also observed in some experiments. The viscosity of the injected phase (displacing phase) increased by the formation of oil-in-water emulsions in which a piston-like displacement occurred for the fluid bulk (Pei et al. 2015; Zhang et al. 2010). It is expected that the surface charge density of existing cations in seawater increased with a decrease in the atomic radius, and higher amounts of asphaltene were absorbed which resulted in an interfacial tension reduction (Maaref et al. 2017). According to the mechanism of the salting-in effect and theory of Derjaguin–Landau–Verwey–Overbeek (DLVO), the disjoining pressure increased and charged surfaces distanced each other and nanoparticles were located preferentially at the interface of two fluids and stabilized the emulsion molecules by reducing the interfacial tension (Lashkarbolooki et al. 2016). Also, higher interactions among asphaltene molecules occurred with an increase in the number of free ions and anions in which the stability increased because the asphaltene molecules have multiple active electronegative sites such as –OH, =C=O and =N (Lashkarbolooki et al. 2016). These chemical bonds strongly tend to absorb protons, and it is possible for negatively charged asphaltene molecules to be absorbed onto H^+ ions and become positive loads (Lashkarbolooki et al. 2016; Shojaati et al. 2017). As a result of low and high pH values, functional groups of asphaltene are charged and result in higher polarity and hydrophilicity that increase the stability. It is essential to precisely observe the mechanisms in all the injections and determine the reason for the final recovery changes. The breakthrough time of each displacing sample is presented in Fig. 10.

Figure 10 shows that the Fe_3O_4/SiO_2 nanocomposite has the longest breakthrough time which means a relatively long

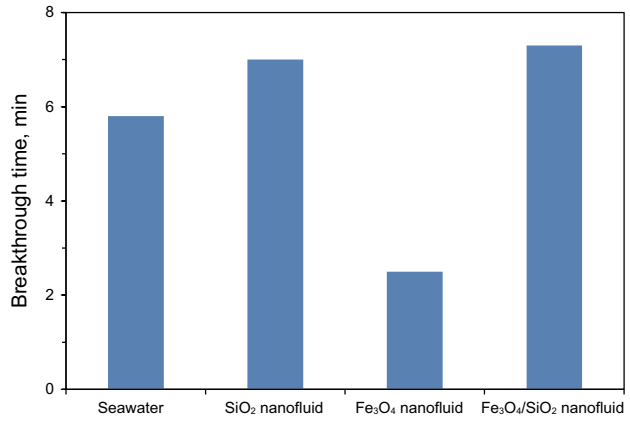

Fig. 10 Breakthrough time of each displacing fluid

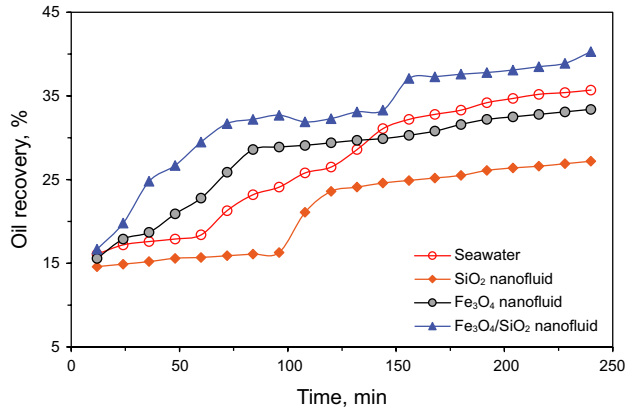

Fig. 11 Recovery as a function of injection time for four displacing fluids

time required for this nanofluid before the first droplet of water drains from the micromodel output. Oxide nanoparticles have high absorption potentials for asphaltenes on their surfaces due to their high specific surface area (SSA) values. This also leads to an increase in viscosity apart from its effect on increasing the stability of asphaltene molecules which creates piston-like motions in both low- and high-permeability zones due to forming a pressure resistance in the environment. Moreover, acidic nanoparticles have more power due to creating electrostatic repulsion between two surfaces of the fluids which dominates the capillary forces and van der Waals disjoining pressures that lead to more piston-like motion and higher production. Greater sweeping and piston-like flow motion were detected in fluids by the increase in the breakthrough time that enhances the efficiency of oil recovery. The Fe_3O_4 nanofluid has the shortest breakthrough time among all the displacing fluids due to the weakness of oxide nanoparticles to overcome van der Waals disjoining pressure in which they are displaced by the incoming pressure waves of the fluid injection and can alter the wettability poorly. These nanoparticles thus find a quick way to the micromodel output instead of remaining in the micromodel and moving the fluid toward the exit point.

As shown in Fig. 11, the Fe_3O_4/SiO_2 nanocomposite has the best performance in enhanced oil recovery than others. Not only does this nanocomposite remain in the porous medium with a high breakthrough time leading to oil production, but also there are some oscillations in the reported recovery that could be due to several reasons like emulsion production or producing as a slug or image-processing accuracy. It is worth noting that it has a high capability in altering the wettability of the system. As it can be seen from the oil-saturated micromodel, it is an oil-wet system. Nanoparticles can alter the wettability to water wet according to Fig. 12 by locating on the surface of the glass (Ehtesabi et al. 2014). Hydrophilic nanoparticles can enhance the stability in addition to increasing the electrostatic double-layer repulsion force and drive the system toward higher water-wet conditions as the concentration and capacity of electrolytes increase in the environment.

Wettability alteration from oil wet to water wet results in a release of oil toward the exit and production. It thus can be seen from Fig. 11 that the final recovery of Fe_3O_4/SiO_2 injection is 40.3% while its value is 12.9% for distilled water injection. As it can be observed from Fig. 11, Fe_3O_4 and SiO_2 nanofluids have lower final recoveries than the seawater. This is due to the properties of nanoparticles in absorbing asphaltene for activating EOR mechanisms. Also, SiO_2 nanoparticles may react more easily with water and release their surface silanol groups (SiOH) to increase the stability of asphaltene molecules as the salinity of the aqueous phase decreases in the system. The governing mechanism in oil recovery by injecting the Fe_3O_4 nanofluid is the controlling of asphaltene precipitation. As it has also been mentioned in previous studies (Doryani et al. 2015, 2016), these nanoparticles decrease the precipitation of asphaltenes on the glass by adsorbing asphaltene particles on their surfaces so less blockage of throats by precipitation is detected. Consequently, a reduction in asphaltene precipitation was observed by this injection while other mechanisms are active too (Fig. 13).

The SiO_2 nanofluid can produce oil by reducing the interfacial tension and altering wettability. SiO_2 nanoparticles are not capable of reducing the interfacial tension by themselves due to the lack of surface activity; however, the presence of extra electrolytes including cations in seawater and polar compounds in oil such as asphaltene and resin can enhance the surface activity of these nanoparticles and reduce the interfacial tension. Wettability alteration is also attributed to the existence of polar compounds in oil, with mechanisms of typical crude oil components with polar functionality, surface precipitation and ion-bonding mechanisms of cations. The final oil recovery of the SiO_2 nanofluid in this injection

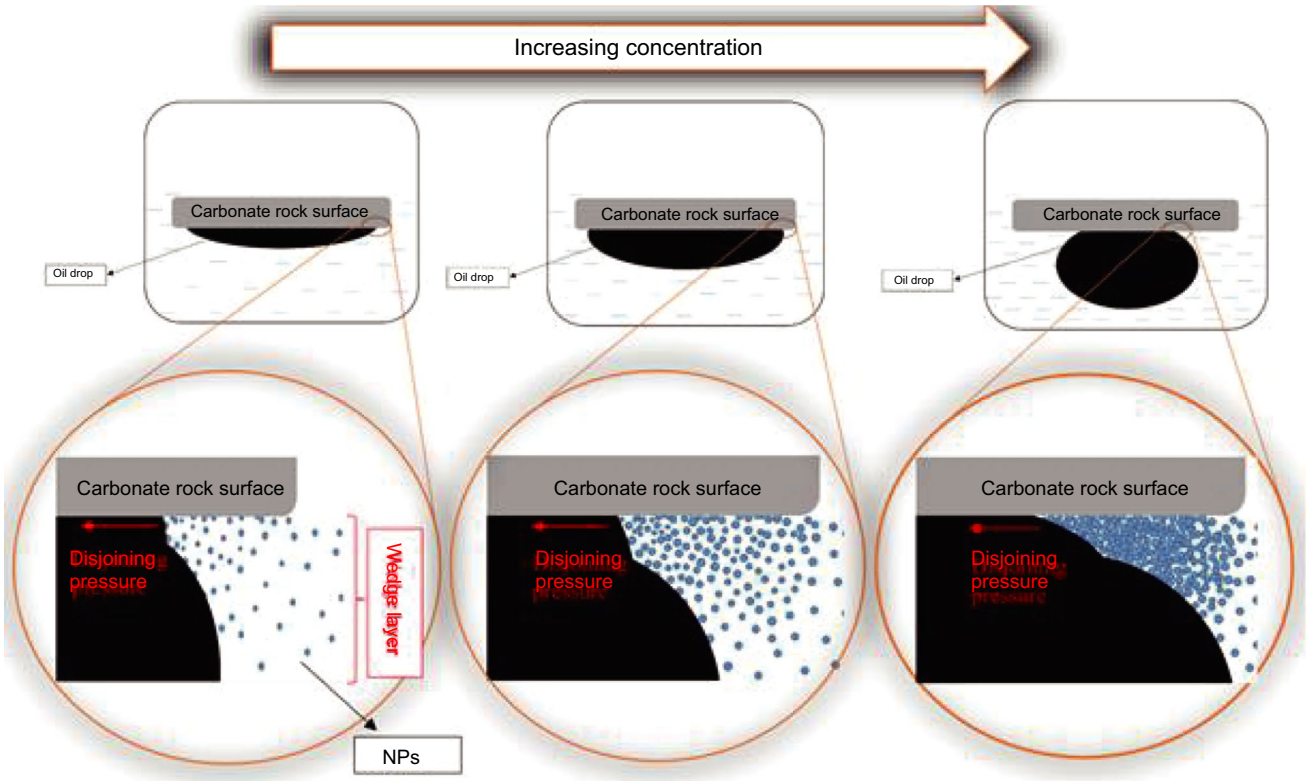

Fig. 12 Schematic view of wettability alteration by nanofluid (Ehtesabi et al. 2014)

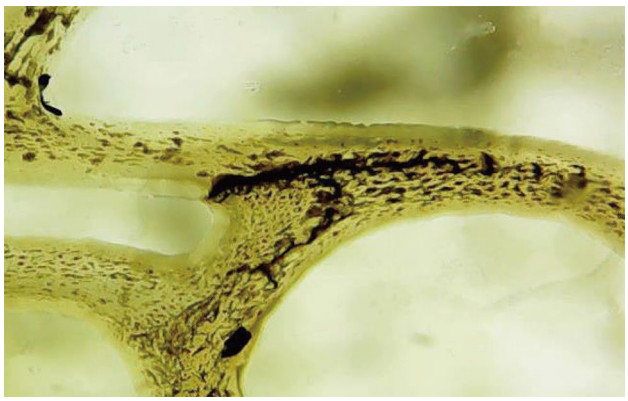

Fig. 13 Asphaltene precipitation during water injection without nanoparticles

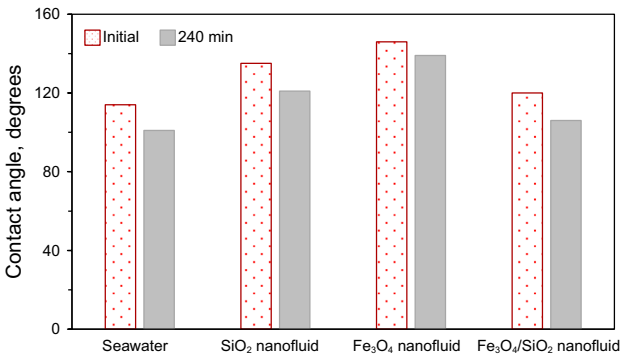

Fig. 14 Contact angle of the glass in contact with all four displacing fluids and the utilized oil at the initial moment and after 240 min

is, therefore, lower than other nanofluids and seawater. Wettability of the glass was evaluated in the presence of the displacing fluids and the oil sample by measuring contact angle for about 240 min of aging. Glass wettability for all the four fluids is shown in Fig. 14 at both the initial moment and after 240 min of aging.

By injecting the Fe_3O_4/SiO_2 nanofluid into the micromodel, it can be observed that not only asphaltene precipitation is reduced but also the wettability is altered to neutral. As it can be observed from Fig. 14, the values of contact angle for seawater, SiO_2, Fe_3O_4 and Fe_3O_4/SiO_2 nanofluids are 101°, 121°, 139° and 106°, respectively. The glass changed from oil wet to neutral. According to $p_c = \frac{2\sigma\cos\theta}{r}$, because of the approaching of θ to 90°, p_c approaches zero. The equilibrium interfacial tension (IFT) was measured, and the values for seawater, SiO_2, Fe_3O_4 and Fe_3O_4/SiO_2 nanofluids were 25, 24, 26 and 21 mN/m, respectively. The IFT reduced when the nanoparticles/

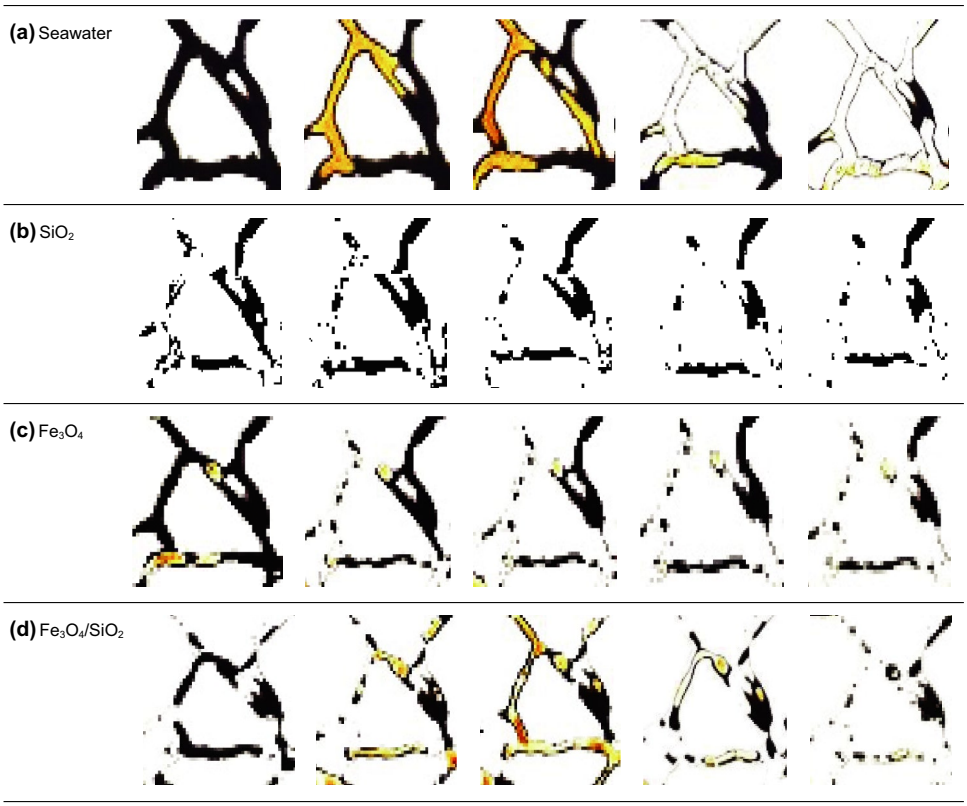

Fig. 15 A part of the micromodel (includes pores and throats) for four displacing fluids at the same times after injection

nanocomposites were introduced into the system. The main mechanism is the movement and placement of nanoparticles on oil and water surfaces. As a matter of fact, because of the presence of nanoparticles on the surface, the asphaltene adsorption would be more and the interfacial viscosity will be higher due to the presence of natural surfactant (asphaltene). Therefore, the IFT decreases (Maurya et al. 2017; Maurya and Mandal 2018). Aside from all the mentioned mechanisms, it is also observed that the Fe_3O_4/SiO_2 nanofluid is helpful for the formation of stable emulsions in the porous medium. These stable emulsions can enhance the viscosity of the displacing fluid to higher than the existing oil so that the fluid may sweep more oil trapped in pores and drive oil to the micromodel exit. Emulsions can thicken the film layer around the oil droplets through the mechanism of pseudo-emulsion film theory and improve the stability of emulsions due to lowering the interfacial tension and raising viscosity. Furthermore, viscous fingering is diminished by increasing the viscosity of the displacing fluid and reducing the viscosity difference between the displacing fluid and oil in the medium, which results in a piston-like motion of the displacing fluid and an enhancement in recovery. A part of the micromodel during the separate injection of four fluids at the same times after injection is illustrated in Fig. 15. The brown color shows the formation of oil-in-water emulsions.

The water injected will increase by creating water-in-oil emulsion in the front of the fluid injected, and the mobility ratio will improve. Because of the emulsion formation, the oil drops stick together and become larger, and this causes an increase in the oil mobility. Also, due to the emulsion formation, the high-permeability zones are blocked and the sweep efficiency is increased (Kumar et al. 2017; Maurya and Mandal 2018). According to Fig. 15, the formation of emulsions was detected in the injection of all fluids but at different injection times, however, in the injection of the Fe_3O_4/SiO_2 nanofluid, the stability of emulsions was observed from the beginning of the injection until the end. Although the emulsion formation is sometimes significantly increased due to the existence of ions listed in Table 3, its stability is limited as it forms in a certain time and is degraded afterward. This is primarily because not all the ions in seawater act in favor of emulsion formation and stabilization, but disturbing ions can neutralize the effect of other ions which have reacted with asphaltene and destroy the emulsion not very long after its formation. The Fe_3O_4/SiO_2 nanofluid, however, acts in favor of emulsion formation in which the effects of favoring factors dominate the opposing factors.

4 Conclusions

In this study, seawater and different nanofluids (Fe_3O_4, SiO_2 and Fe_3O_4/SiO_2 in seawater) were investigated and analyzed for enhancing oil recovery. Experiments were conducted at ambient conditions. Experimental results show that the 0.1 wt% Fe_3O_4/SiO_2 nanofluid has the highest final oil recovery. The governing mechanism in oil recovery enhanced by the Fe_3O_4/SiO_2 nanofluid is the rapid wettability alteration in the porous medium. The Fe_3O_4 nanofluid recovered oil mostly by controlling asphaltene precipitation in such a way, and the final recovery increased by 13.2% compared to distilled water injection. The SiO_2 nanofluid affects wettability alteration and IFT reduction. Seawater can also alter wettability, reduce the interfacial tension, control asphaltene precipitation and give rise to unstable emulsions forming due to its active ions. Among the injected fluids, the synthesized Fe_3O_4/SiO_2 nanofluid not only alters the wettability and reduces the asphaltene precipitation by forming stable oil-in-water emulsions, but also increases the viscosity of the displacing fluid. Formation of stable emulsions can increase oil production and enhance the final oil recovery up to about two times more than distilled water. Accordingly, all four fluids can generally be sorted with respect to their final oil recovery values as follows: Fe_3O_4/SiO_2 > seawater > Fe_3O_4 > SiO_2. It must be mentioned that the utilized oil is susceptible to asphaltene precipitation, and hence, controlling its precipitation by adsorption on the surfaces of the nanoparticles or existing ions in fluids plays an important role in the final oil recovery. Properties of the utilized oil are therefore considered in screening the displacing fluids.

References

Ahmadi MA, Ahmad Z, Phung LTK, Kashiwao T, Bahadori A. Evaluation of the ability of the hydrophobic nanoparticles of SiO2 in the EOR process through carbonate rock samples. Pet Sci Technol. 2016;34(11–12):1048–54. https://doi.org/10.1080/10916466.2016.1148052.

Al-Anssari S, Barifcani A, Wang S, Maxim L, Iglauer S. Wettability alteration of oil-wet carbonate by silica nanofluid. J Colloid Interface Sci. 2016;461:435–42. https://doi.org/10.1016/j.jcis.2015.09.051.

Al Adasani A, Bai B. Analysis of EOR projects and updated screening criteria. J Pet Sci Eng. 2011;79(1–2):10–24. https://doi.org/10.1016/j.jcis.2015.09.051.

Aminzadeh B, Chung D, Zhang X, Bryant S, Huh C, DiCarlo D. Influence of surface-treated nanoparticles on displacement patterns during CO_2 injection. In: SPE annual technical conference and exhibition, 30 September–2 October, New Orleans, Louisiana, USA; 2013. https://doi.org/10.2118/166302-MS.

Bera A, Belhaj H. Application of nanotechnology by means of nanoparticles and nanodispersions in oil recovery—a comprehensive review. J Nat Gas Sci Eng. 2016;34:1284–309. https://doi.org/10.1016/j.jngse.2016.08.023.

Cheraghian G, Hendraningrat L. A review on applications of nanotechnology in the enhanced oil recovery part A: effects of nanoparticles on interfacial tension. Int Nano Lett. 2016a;6(2):129–38. https://doi.org/10.1007/s40089-015-0173-4.

Cheraghian G, Hendraningrat L. A review on applications of nanotechnology in the enhanced oil recovery part B: effects of nanoparticles on flooding. Int Nano Lett. 2016b;6(1):1–10. https://doi.org/10.1007/s40089-015-0170-7.

Doryani H, Kazemzadeh Y, Parsaei R, Malayeri M, Riazi M. Impact of asphaltene and normal paraffins on methane-synthetic oil interfacial tension: an experimental study. J Nat Gas Sci Eng. 2015;26:538–48. https://doi.org/10.1016/j.jngse.2015.06.048.

Doryani H, Malayeri M, Riazi M. Visualization of asphaltene precipitation and deposition in a uniformly patterned glass micromodel. Fuel. 2016;182:613–22. https://doi.org/10.1016/j.fuel.2016.06.004.

Doryani H, Malayeri M, Riazi M. Precipitation and deposition of asphaltene in porous media: impact of various connate water types. J Mol Liq. 2018;258:124–32. https://doi.org/10.1016/j.molliq.2018.02.124.

Ehtesabi H, Ahadian MM, Taghikhani V. Enhanced heavy oil recovery using TiO_2 nanoparticles: investigation of deposition during transport in core plug. Energy Fuels. 2014;29(1):1–8. https://doi.org/10.1021/ef5015605.

El-Diasty AI, Aly AM. Understanding the mechanism of nanoparticles applications in enhanced oil recovery. In: SPE North Africa technical conference and exhibition, 14-16 September, Cairo, Egypt; 2015. https://doi.org/10.2118/175806-MS.

Hendraningrat L, Li S, Torsaeter O. Enhancing oil recovery of low-permeability Berea sandstone through optimised nanofluids concentration. In: SPE enhanced oil recovery conference, 2–4 July, Kuala Lumpur, Malaysia; 2013. https://doi.org/10.2118/165283-MS.

Kazemzadeh Y, Eshraghi SE, Kazemi K, Sourani S, Mehrabi M, Ahmadi Y. Behavior of asphaltene adsorption onto the metal oxide nanoparticle surface and its effect on heavy oil recovery. Ind Eng Chem Res. 2015;54(1):233–9. https://doi.org/10.1021/ie503797g.

Kazemzadeh Y, Sharifi M, Riazi M. Mutual effects of Fe_3O_4/chitosan nanocomposite and different ions in water for stability of water-in-oil (W/O) emulsions at low–high salinities. Energy Fuels. 2018a;32(12):12101–17. https://doi.org/10.1021/acs.energyfuels.8b02449.

Kazemzadeh Y, Sharifi M, Riazi M, Rezvani H, Tabaei M. Potential effects of metal oxide/SiO_2 nanocomposites in EOR processes at different pressures. Colloids Surf A. 2018b;559:372–84. https://doi.org/10.1016/j.colsurfa.2018.09.068.

Kazemzadeh Y, Shojaei S, Riazi M, Sharifi M. Review on application of nanoparticles for EOR purposes: a critical of the opportunities and challenges. Chin J Chem Eng. 2018c. https://doi.org/10.1016/j.cjche.2018.05.022.

Krevor S, Blunt MJ, Benson SM, Pentland CH, Reynolds C, Al-Menhali A, Niu B. Capillary trapping for geologic carbon dioxide storage–From pore scale physics to field scale implications. Int J Greenhouse Gas Control. 2015;40:221–37. https://doi.org/10.1016/j.ijggc.2015.04.006.

Kumar A, Mandal A. Characterization of rock–fluid and fluid–fluid interactions in presence of a family of synthesized zwitterionic

surfactants for application in enhanced oil recovery. Colloids Surf A. 2018;549:1–12. https://doi.org/10.1016/j.colsurfa.2018.04.001.
Kumar N, Gaur T, Mandal A. Characterization of SPN Pickering emulsions for application in enhanced oil recovery. J Ind Eng Chem. 2017;54:304–15. https://doi.org/10.1016/j.jiec.2017.06.005.
Lashkarbolooki M, Riazi M, Ayatollahi S, Hezave AZ. Synergy effects of ions, resin, and asphaltene on interfacial tension of acidic crude oil and low–high salinity brines. Fuel. 2016;165:75–85. https://doi.org/10.1016/j.fuel.2015.10.030.
Li Q, Wei B, Lu L, Li Y, Wen Y, Pu W, Li H, Wang C. Investigation of physical properties and displacement mechanisms of surface-grafted nano-cellulose fluids for enhanced oil recovery. Fuel. 2017;207:352–64. https://doi.org/10.1016/j.fuel.2017.06.103.
Liu K-L, Kondiparty K, Nikolov AD, Wasan D. Dynamic spreading of nanofluids on solids part II: modeling. Langmuir. 2012;28(47):16274–84. https://doi.org/10.1021/la302702g.
Maaref S, Ayatollahi S, Rezaei N, Masihi M. The effect of dispersed phase salinity on water-in-oil emulsion flow performance: a micromodel study. Ind Eng Chem Res. 2017;56(15):4549–61. https://doi.org/10.1021/acs.iecr.7b00432.
Maurya NK, Kushwaha P, Mandal A. Studies on interfacial and rheological properties of water soluble polymer grafted nanoparticle for application in enhanced oil recovery. J Taiwan Inst Chem Eng. 2017;70:319–30. https://doi.org/10.1016/j.jtice.2016.10.021.
Maurya NK, Mandal A. Investigation of synergistic effect of nanoparticle and surfactant in macro emulsion based EOR application in oil reservoirs. Chem Eng Res Des. 2018;132:370–84. https://doi.org/10.1016/j.cherd.2018.01.049.
Moghadam TF, Azizian S. Effect of ZnO nanoparticles on the interfacial behavior of anionic surfactant at liquid/liquid interfaces. Colloids Surf A. 2014;457:333–9. https://doi.org/10.1016/j.colsurfa.2014.06.009.
Nassar NN, Hassan A, Pereira-Almao P. Application of nanotechnology for heavy oil upgrading: catalytic steam gasification/cracking of asphaltenes. Energy Fuels. 2011a;25(4):1566–70. https://doi.org/10.1021/ef2001772.
Nassar NN, Hassan A, Pereira-Almao P. Effect of the particle size on asphaltene adsorption and catalytic oxidation onto alumina particles. Energy Fuels. 2011b;25(9):3961–5. https://doi.org/10.1021/ef2008387.
Ogolo N, Olafuyi O, Onyekonwu M. Enhanced oil recovery using nanoparticles. In: SPE Saudi Arabia section technical symposium and exhibition, 8-11 April, Al-Khobar, Saudi Arabia; 2012. https://doi.org/10.2118/160847-MS.
Parsaei R, Kazemzadeh Y, Abadshapoori AK, Riazi M. Study of asphaltene precipitation during CO_2 injection to oil reservoirs in the presence of iron oxide nanoparticles by interfacial tension and bond number measurements. In: 79th EAGE conference and exhibition; 2017.
Patel A, Nihalani D, Mankad D, Patel D, Chaudhari R, Dhameliya M, Tripathi D, Bhui UK. Evaluating feasibility of hydrophilic silica nanoparticles for in situ emulsion formation in presence of Co-surfactant: an experimental study. In: SPE Kingdom of Saudi Arabia annual technical symposium and exhibition, 24–27 April, Dammam, Saudi Arabia; 2017. https://doi.org/10.2118/188141-MS.
Pei H, Zhang G, Ge J, Zhang J, Zhang Q, Fu L. Investigation of nanoparticle and surfactant stabilized emulsion to enhance oil recovery in waterflooded heavy oil reservoirs. In: SPE Canada heavy oil technical conference, 9–11 June, Calgary, Alberta, Canada; 2015. https://doi.org/10.2118/174488-MS.
Pourabdollah K, Moghaddam AZ, Kharrat R, Mokhtari B. An experimental feasibility study of in situ nano-particles in enhanced oil recovery and heavy oil production. Energy Sources Part A Recovery Util Environ Effects. 2013;35(23):2198–208. https://doi.org/10.1080/15567036.2010.527903.
Rezvani H, Riazi M, Tabaei M, Kazemzadeh Y, Sharifi M. Experimental investigation of interfacial properties in the EOR mechanisms by the novel synthesized Fe_3O_4@chitosan nanocomposites. Colloids Surf A. 2018;544:15–27. https://doi.org/10.1016/j.colsurfa.2018.02.012.
Roustaei A, Moghadasi J, Bagherzadeh H, Shahrabadi A. An experimental investigation of polysilicon nanoparticles' recovery efficiencies through changes in interfacial tension and wettability alteration. In: SPE international oilfield nanotechnology conference and exhibition, 12–14 June, Noordwijk, The Netherlands; 2012. https://doi.org/10.2118/156976-MS.
Sharma T, Kumar GS, Chon BH, Sangwai JS. Thermal stability of oil-in-water Pickering emulsion in the presence of nanoparticle, surfactant, and polymer. J Ind Eng Chem. 2015;22:324–34. https://doi.org/10.1016/j.jiec.2014.07.026.
Shojaati F, Mousavi SH, Riazi M, Torabi F, Osat M. Investigating the effect of salinity on the behavior of asphaltene precipitation in the presence of emulsified water. Ind Eng Chem Res. 2017;56(48):14362–8. https://doi.org/10.1021/acs.iecr.7b03331.
Skauge T, Spildo K, Skauge A. Nano-sized particles for EOR. In: SPE improved oil recovery symposium, 24–28 April, Tulsa, Oklahoma, USA; 2010. https://doi.org/10.2118/129933-MS.
Steeb H, Kurzeja PS, Frehner M, Schmalholz SM. Phase velocity dispersion and attenuation of seismic waves due to trapped fluids in residual saturated porous media. Vadose Zone J. 2012;11(3):vzj2011.0121. https://doi.org/10.2136/vzj2011.0121.
Suleimanov B, Ismailov F, Veliyev E. Nanofluid for enhanced oil recovery. J Pet Sci Eng. 2011;78(2):431–7. https://doi.org/10.1016/j.petrol.2011.06.014.
Wang KL, Liang SC, Wang CC. Research of improving water injection effect by using active SiO_2 nano-powder in the low-permeability oilfield. In: Advanced Materials Research, vol 92. Trans Tech Publications; 2010. pp. 207–12. https://doi.org/10.4028/www.scientific.net/AMR.92.207.
Wei B, Li Q, Jin F, Li H, Wang C. The potential of a novel nanofluid in enhancing oil recovery. Energy Fuels. 2016;30(4):2882–91. https://doi.org/10.1021/acs.energyfuels.6b00244.
Zhang T, Davidson D, Bryant SL, Huh C. Nanoparticle-stabilized emulsions for applications in enhanced oil recovery. In: SPE improved oil recovery symposium, 24–28 April, Tulsa, Oklahoma, USA; 2010. https://doi.org/10.2118/129885-MS.
Zhang C, Oostrom M, Wietsma TW, Grate JW, Warner MG. Influence of viscous and capillary forces on immiscible fluid displacement: pore-scale experimental study in a water-wet micromodel demonstrating viscous and capillary fingering. Energy Fuels. 2011;25(8):3493–505. https://doi.org/10.1021/ef101732k.